



Multi-objective optimization and characterization of cylindricity and material removal rate in nanographene mixed dielectric EDM using ANFIS and MOSOA

ASHISH GOYAL, DEEPESH SHARMA, ARNAB BHOWMICK and
VIMAL KUMAR PATHAK*

Department of Mechanical Engineering, Manipal University Jaipur, Jaipur, Rajasthan, India
e-mail: vimalpthk@gmail.com

MS received 4 August 2021; revised 14 February 2022; accepted 1 June 2022

Abstract. The current study performed modeling, analysis, and optimization of electrical discharge machining (EDM) under nano graphene mixed dielectric machining of Inconel 718 using ANFIS and a newly developed multi-objective seagull optimization algorithm. The influence of three major EDM controlling parameters namely peak current (I_p), pulse on time (T_{on}), and pulse off time (T_{off}) have been studied on the output machining characteristics viz. material removal rate (MRR) and cylindricity (CY) deviation for each of the experiments. In this work, EDM performance was enhanced by dispersing nano-graphene powder into EDM Oil as a dielectric medium and improvement from conventional EDM was analysed. The Taguchi L27 orthogonal array was utilized for planning and conducting EDM experiments, while analysis of variance (ANOVA) tests and regression analysis were conducted for examining the influence of input process variables on machining response variables. From results, it was realized that nano graphene mixed dielectric EDM improved the machining performance in comparison to traditional EDM performance. The modeling of response variables in terms of input process variables and optimal process conditions were determined using efficient intelligent methods namely ANFIS model and the newly developed multi-objective seagull optimization algorithm (MOSOA), respectively. It was found that nanographene mixed EDM improved MRR and cylindricity deviation by 13.88% and 25.76% respectively in comparison to conventional EDM without nanographene mixed dielectric. The MOSOA algorithm provides a number of non-dominated pareto solutions and best machining conditions among 32 optimal sets for nanographene mixed EDM was selected as a pulse on time of 12 μ s, pulse off time as 7 μ s, and peak current at 9 A. Finally, the scanning electron microscopy image also shows the improvement in surface finish of nano graphene mixed dielectric EDM in comparison to traditional EDM.

Keywords. Cylindricity deviation; MRR; nanographene; powder mixed EDM; ANFIS modeling; MOSOA.

1. Introduction

The use of nickel-based superalloy namely Inconel 718 have gained significant interest among different industries owing to its excellent mechanical properties including high strength, toughness, corrosion resistance and fatigue resistance along with high strength to weight ratio [1]. The machining of such superalloys becomes challenging using conventional material removal process because of chip breaking, higher temperature at tool tip, formation of built-up edge, burr formation and high tool wear [2]. Thus, need of a versatile and non-conventional material removal process leads to the emergence of electrical discharge machining (EDM), which has higher efficacy in overcoming the aforementioned challenges [3]. Since its inception,

EDM has been widely employed to produce complicated shapes like cavities, contours, geometric features, intricate patterns with greater precision and accuracy, unlike traditional machining processes. In addition, EDM offers various advantages with numerous applications like manufacturing of molds, tools and dies, automotive, aerospace, and surgical products [4]. EDM is an electro-thermal machining process that utilizes a series of electrical sparks occurring between electrodes, submerged into a dielectric medium to undergo a material erosion process. The sparks are produced once the applied voltage surpasses the threshold value [5]. Almost all electrically conductive materials irrespective of their strength, hardness, and toughness can be machined with better dimensional control through the EDM process [6].

In the past, several works have been performed for enhancing the machining efficiency and productivity of

*For correspondence
Published online: 12 July 2022

conventional EDM process [7, 8]. In this context, research work was carried out concentrated on changing the tool electrodes [9], applying outer magnetic field [10], use of deionized water dielectric [11] and rotating the tool electrode [12], etc. The change in tool electrodes minimizes the tool wear, thus improves the productivity. The rotation of tool with ultrasonic vibrations provides enhanced MRR and surface finish of workpiece by efficiently minimizing the debris from machining zone [13, 14]. The application of water ionized dielectric provides health safety to the operator and environment as well and minimized tool wear [15]. These modifications in EDM provides enhanced machining efficacy and productivity in industries however involves some drawbacks such as more tool rotation can cause material removal rate to decrease owing to lower ionization energy [16]. Similarly, magnetic field induced EDM is valid for low magnetic field and can improved material removal rate to a certain level only [17]. Some of the cases involve arc instability during machining, however a recent variant of EDM overcomes most of these shortcomings by adding nano particles in dielectric medium and thus stability of created spark can be realized during machining of workpiece [18].

Several research works have been conducted on utilizing nano particle mixed EDM (NPEDM) as an adequate modification of conventional EDM. In NPEDM, superior machining performance can be achieved owing to its improvement in the spark stability, frequency, and thermal conductivity at the machining zone. In addition, the tool workpiece gap condition improves significantly realizing better surface finish of the workpiece [19]. Researchers utilized different nanoparticles mixed with dielectric fluid for EDM process, thus improving the machining characteristics in terms of MRR, TWR, surface roughness, recast layer, etc. [20, 21]. The nano particles applied for dispersion in dielectric fluid includes TiO_2 , Al, Al_2O_3 , W, SiC, Cr, CNT, Gr/C, Mo, and Cu for enhancing the electric field intensity and achieving better flushing at the machining zone [4]. Surekha *et al* investigated the influence of adding aluminium powder in dielectric fluid on MRR and tool wear rate during EDM of EN-19 alloy steel. It was revealed from results that MRR was increased significantly by utilizing aluminium powder dielectric fluid after peak current [22]. Paswan *et al* realized improvement in material removal rate, surface roughness, and tool wear rate by 20.1%, 14%, and 2% respectively due to stable sparking between electrodes during machining of Inconel 718 superalloy utilizing graphene nanofluid in the dielectric medium [23]. Baseri *et al* significantly improved the material removal rate using TiO_2 nano powder mixed dielectric EDM up to 1 g/l concentration along with a rotary tool [24]. The use of higher TiO_2 nanopowder concentration minimizes the debris deposition at the machining zone by facilitating adequate flushing thus improves surface finish also.

Kumar *et al* studied the effect of adding silicon powder in kerosene oil dielectric medium for EDM of EN-24 tool steel and performed multi-objective optimization for minimizing surface roughness and maximizing MRR. Results revealed that silicon powder concentration comes out as the most significant parameters affecting the response machining characteristics followed by peak current and pulse on time [25]. Sivaprakasam *et al* explored the influence of mixing graphite nanopowder in dielectric for performing EDM on Inconel alloy. It was observed that the suspended nanographite powders resulted in uniform distribution of sparks thus improving surface finish due to widened plasma channel [26]. Kumar *et al* revealed that mixing of Al_2O_3 nanopowder with deionized water during EDM of Inconel 825 workpiece provides reduced micro-cracks, higher machining stability, reduction in short-circuiting, and enhanced surface topography in comparison to conventional EDM [27]. Sari *et al* employed MWCNT mixed dielectric for improving the machining characteristics during EDM of AISI H13 tool steel. It was found from the results that MWCNT mixed dielectric EDM provides smaller recast layer thickness and enhanced surface finish in comparison to conventional EDM processing. The primary reason of the higher removal rate being higher thermal conductivity of MWCNT particles thus removing heat at a faster rate in the machining zone [28]. Yeo *et al* applied SiC nanoparticles mixed dielectric and their work results in reduction in the flow of charges between electrodes, which establishes consistent depth with smaller crater size, thus enhances the surface finish effectively in comparison to conventional EDM [29].

Similarly, Prihandana *et al* investigated different sizes of Molybdenum disulphide (MoS_2) powder suspended in the dielectric fluid to improve the machining performance of micro-EDM during the processing Inconel 718. It was revealed that 50 nm particle size of MoS_2 powder provides maximum value of material removal rate during PMEDM of Inconel 718 [30]. Tiwary *et al* studied effect of three different conducting powders mixed deionized water dielectric on the tool wear rate, overcut and surface roughness during Micro-EDM of titanium alloy. Based on multi-objective optimization, the study recommended copper powder mixed dielectric as best choice for realizing desired responses [31]. HuuPhan *et al* in their study explored the surface quality of workpiece using different materials EDM electrodes and titanium powder mixed dielectric medium. The results revealed that copper electrode with titanium powder mixed EDM provides a harder surface and enhanced surface quality [32]. Prabhu *et al* analyzed the surface roughness for carbon nanotube mixed dielectric EDM of AISI D2 steel using adaptive neuro fuzzy inference system (ANFIS) model and modelled the surface roughness with an accuracy of 97.53% [33]. Cogun *et al* investigated experimentally different surface characteristics

along with microstructure change for EDM of prismatic steel sample utilizing boric acid mixed dielectric medium. The work recommended that powder concentration and pulse time are significant factors that affected machining efficiency [34].

Recently, various intelligent and statistical approaches were employed to investigate the experimental results for prediction and optimization of the output characteristics to enhance the machining performance. Abhilash *et al* developed an artificial neural network (ANN) model during wire-EDM machining of Inconel 718 to analyze and predict the influence of pulse-on time, pulse-off time, servo voltage, and wire feed rate on machining failures such as spark absence and wire breakage [35]. Jafarian *et al* studied the effects of input variables viz. voltage, pulse-on time, peak current, and pulse-off time on the material removal rate and surface quality using ANN-NSGA-II methodology while EDM machining of Inconel 718 alloy [36]. Sengottuvel *et al* employed the Fuzzy Logic Methodology for precise and easy selection of EDM input parameters and optimizing multiple characteristics like MRR, TWR, and SR, achieving 95% accuracy during machining of Inconel 718 [37]. Ashok *et al* utilized Fuzzy logic and ANN technique while evaluating MRR and proposed that Fuzzy logic exhibited better optimization results for aluminium alloy hybrid nanocomposites machined through Wire-EDM [38].

The machined surface is required to be in adequate dimensional and geometric control for its enhanced functional performance. The EDM application in moulds, dies, tools and presswork operation are focused to manufacture components with precised and defined tolerances with minimum cost. Dhanabalan *et al* optimized machining characteristics like MRR, EWR, straightness, perpendicularity, and angularity of square and hexagonal holes on Inconel 718 machined through EDM using Taguchi method based grey analysis [39]. Optimization methods such as GRA and Fuzzy logic were applied to predict the influence of dominating process variables on machining responses viz. MRR, EWR, circularity, and cylindricity after Inconel 718 EDM machining using different electrodes [40]. Senthilkumar *et al* inferred that peak current was the most deciding process parameter with 69.08% for EDM machining of hybrid metal matrix composite by employing the GRA method for optimization of circularity, cylindricity, perpendicularity, and radial overcut [41].

Thus, from the above research survey, it is evident that substantial work has been done till date using nanopowder mixed EDM (NPEDM) for analysing the surface roughness, MRR, tool wear rate and recast layer on dissimilar materials and composites, however no substantial work is available for examining form error i.e., cylindricity, for nano-graphene mixed dielectric EDM during processing of Inconel 718 workpiece. The form error like cylindricity needs to be controlled during manufacturing to carry out the desired function correctly as it greatly affects the performance of components, especially in assemblies. In

addition, the influence of nanographene powder mixed dielectric has not been studied appropriately for multi-objective optimization of EDM process variables in minimizing cylindricity and maximizing MRR simultaneously during machining Inconel 718 workpiece. For performing multi-objective optimization in current study, a newly developed multi-objective seagull optimization algorithm (MOSOA) is considered that generates a series of pareto optimal solutions. Finally, the ANFIS model is developed for examining and validating optimal results found experimentally and using MOSOA.

2. Material and methods

2.1 Experimental set-up

The objective of the present research is to understand and investigate the influence of nanographene mixed dielectric fluid on EDM performance characteristics in terms of cylindricity (CY) (geometric accuracy) and material removal rate (MRR) in comparison to conventional dielectric EDM, and to determine the optimal combinations of input parameter for multi-variate responses. The ZNC EDM machine (Model S-50-6040) which is a make of Savita Machine Tools Private Limited, connected with servo stabilizer was used for machining of Inconel 718 plate under nano graphene mixed nanofluid dielectric and conventional dielectric medium. Copper was selected as our desired electrode material because it has high thermal and electrical conductivity, cost-effective nature, and provides good resistance against corrosion and wear. Also, copper in comparison with brass and zinc electrodes provides a high surface finish, least radial overcut, and a higher degree of precision [42]. The dimension of copper electrode is shown in figure 1a. Initially, the length and diameter of the copper electrode were 200 mm and 12 mm, respectively. As shown in figure 1b, turning operation through lathe machine was utilized for reducing the diameter of copper electrode to 8 mm till electrode length of 50 mm assuming that the flow of discharge current remains the same for both the cross-sections. Low viscosity EDM oil (DEF-92) was used as the dielectric fluid to conduct the experimental work. This EDM oil as a dielectric medium proved to be a great asset for the experiment as it is odorless, thermal resistant, economical and eliminates arching. The Inconel 718 workpiece plate was selected having dimension of 100 mm X 50 mm x 3 mm as shown in figure 4a. The chemical composition of the Inconel 718 workpiece is given in table 1. The workpiece is connected to the positive polarity while negative polarity is applied to the tool electrode.

Graphene nanoparticles show various advantages over other nanoparticles including larger surface area/volume ratio, higher electrical and thermal conductivity, lower erosion, corrosion and clogging, and substantial energy

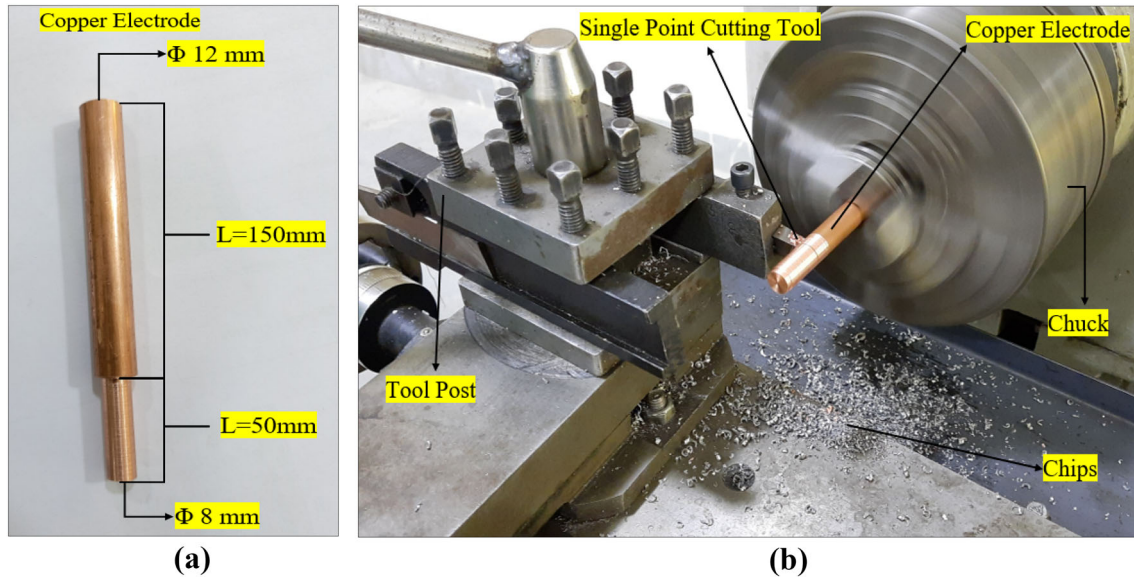


Figure 1. (a) Dimension of copper electrode and (b) Copper electrode machining.

Table 1. Chemical Composition of workpiece Nickel Superalloy Inconel 718.

Element	Ni	Cr	Mo	Nb	Ti
Wt. %	52.76	18.43	2.83	5.12	1.14

saving [43]. Thus, in this work, nanographene was selected to disperse in conventional EDM oil and examine its effect on different response variables. The concentration of graphene nanopowder was selected as 0.5 gm/litre to get a homogenous mixture of nanographene mixed dielectric fluid. A separate machining tank with a capacity of 6 litres was designed to avoid wasting dielectric fluid, choking of the machine filter due to powder particles and to minimize costs. A pump was installed in the newly designed system to ensure proper distribution of dielectric fluid, followed by a stirring mechanism to prevent the powder from settling. In order to carry out the experiment, 3 grams of nanographene powder was added into the dielectric medium i.e., DEF 92 EDM oil as shown in figure 2.

2.2 Process parameters and Taguchi experimental design

In the present work, three predominant control variables such as Peak current (I_p), Pulse-On time (T_{on}), and Pulse-Off time (T_{off}), are selected as the input process parameters

as they greatly influence the performance characteristics of EDM. Output responses i.e., MRR and Cylindricity, have been optimized by analysing the effect of input parameters on varying the values, keeping the other factors constant such as polarity, dielectric pressure at 0.5 kg/cm², and gap voltage of 45 V. The experiments were planned and performed using L27 orthogonal array based on Taguchi's design of experiments (DOE) on MINITAB 19 statistical software. This orthogonal array typically consists of 3 columns and 27 rows producing 27 parametric combinations. These combinations helped to conduct 27 different experiments providing the correlation among the input parameters and response variables. Each input parameter has been allotted three different levels as shown in table 2. In total, 54 experiments were performed, 27 each for two dielectric mediums i.e., EDM Oil and nanographene mixed dielectric. The experimental outcomes have been recorded in table 3.

2.3 Measurement of output responses

Material removal rate (MRR) plays a significant role in exhibiting the performance characteristics of the EDM process. In the present work, MRR is calculated for each machined hole as the difference in weight of the workpiece before and after machining (gm) divided by the machining time (min) and density of the workpiece material. The weight of the workpiece before machining and the weight of the workpiece after machining are measured using an

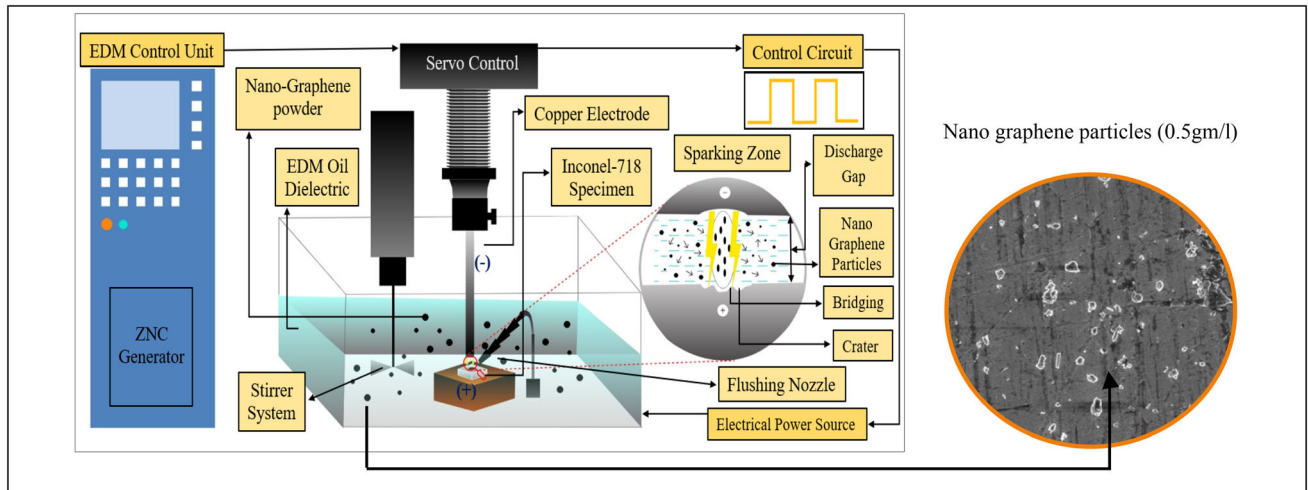


Figure 2. Preparation of nanographene mixed EDM oil in a separate modified tank.

Table 2. Input process parameters and their levels.

Sl. no.	Parameters	Symbol	Level 1	Level 2	Level 3
1.	Peak Current (A)	A	6	9	12
2.	Pulse on time (μs)	B	10	15	20
3.	Pulse off time (μs)	C	7	10	13

Electronic Weighing Balance with 0.1 mg accuracy using Sartorius, model: BSA224S-CW. The MRR was calculated using below eqn.

$$MRR = \frac{W_p - W_a}{t * \rho_w}$$

where W_p and W_a are weight of workpiece prior and after the experiment in grams. ρ_w is the density of workpiece and t is the time taken (minutes) for each turning experiment. The cylindricity is a 3-dimensional tolerance that controls the overall form of a cylinder to ensure that it is round enough and straight enough along its axis. It is a condition of a surface of a revolution in which all points of a surface are equidistant from a common axis [44]. Cylindricity is also known as composite tolerance because it plays a vital role in controlling the circularity and straightness. In this work, cylindricity (CY) was inspected by using a 3-D Coordinate Measuring Machine (CMM) Model TUTOR 5.5.4 made by Accurate Sales and Services Pvt. Cylindricity of the machined holes were measured using the probe attached to the stylus of the CMM machine as shown in figure 3a and b by tracing different positions on the innermost surface of each selected hole machined by two different dielectric mediums. Figure 4 shows the adopted methodology of work conducted from electrical discharge machining of Inconel 718 specimen by addition of

nanographene powder into the EDM oil (DEF-92) to the measurement of response variables and multi-objective optimization using MOSOA.

3. Results and discussions

This section presents the experimentation results based on L_{27} orthogonal array considering different parameter settings under conventional EDM and nanographene mixed EDM processing as in table 3. The outcome of cylindricity and MRR were measured and reported in table 3 for both the cases i.e., with and without nanographene mixed EDM. From the reported experimental results in table 3 for both responses, the minimum-maximum ranges for CY1 and MRR1 are 0.0190–0.0642-mm and 0.87–3.88 mm³/min respectively. The maximum-minimum range for CY2 and MRR2 in case of nanographene mixed EDM are 0.0156–0.0435 mm and 1.04–3.97 mm³/min respectively. It is clearly seen from table 3 that nanographene mixed EDM results outperformed default dielectric EDM results in terms of cylindricity and MRR for corresponding input parameters settings. Tables 4 and 5 reported the analysis of variance (ANOVA) tests for traditional EDM responses i.e., CY1 and MRR1 respectively, for determining how the input parameters influence these responses and percentage contribution of individual parameters. The ANOVA tests were carried out at 95% significance level while higher F-value indicates the significance of input parameters. The ANOVA table for CY1 and MRR1 (without nanographene mixed dielectric EDM) revealed that R² and adjusted R² value comes out above to 91% and 89% respectively, thus showing the significance of the model in predicting these responses. In addition, peak current was found as the most influencing parameter for both the responses of CY1 and MRR1 with percentage contribution of 53.86% and

Table 3. The experimental outcome for the L27 orthogonal array.

Sl. no.	Ton (μ s)	Toff (μ s)	Ip (A)	Without nano graphene dielectric EDM		With nano grapheme dielectric EDM (PMEDM)	
				MRR1 (mm^3/min)	CY1 (mm)	MRR2 (mm^3/min)	CY2 (mm)
1	10	7	6	1.04	0.0296	1.15	0.0245
2	10	7	9	1.98	0.0190	2.02	0.0164
3	10	7	12	3.21	0.0245	2.97	0.0192
4	10	10	6	0.96	0.0365	1.08	0.0302
5	10	10	9	1.84	0.0209	1.96	0.0169
6	10	10	12	2.97	0.0345	3.08	0.0242
7	10	13	6	0.87	0.0389	1.04	0.0297
8	10	13	9	1.70	0.0210	1.91	0.0156
9	10	13	12	2.45	0.0362	2.64	0.0190
10	15	7	6	1.76	0.0421	1.98	0.0277
11	15	7	9	3.11	0.0309	3.39	0.0161
12	15	7	12	3.78	0.0359	3.87	0.0245
13	15	10	6	1.65	0.0480	1.91	0.0250
14	15	10	9	3.08	0.0240	3.21	0.0181
15	15	10	12	3.77	0.0464	3.84	0.0246
16	15	13	6	1.41	0.0495	1.81	0.0368
17	15	13	9	2.87	0.0294	2.74	0.0209
18	15	13	12	2.95	0.0389	2.81	0.0264
19	20	7	6	2.2	0.0515	2.36	0.0435
20	20	7	9	3.18	0.0313	3.40	0.0226
21	20	7	12	3.88	0.0496	3.97	0.0390
22	20	10	6	2.15	0.0642	2.13	0.0509
23	20	10	9	2.93	0.0321	3.04	0.0349
24	20	10	12	3.44	0.0520	3.10	0.0411
25	20	13	6	2.09	0.0569	2.26	0.0428
26	20	13	9	2.56	0.0313	2.98	0.0364
27	20	13	12	3.12	0.0468	3.31	0.0410

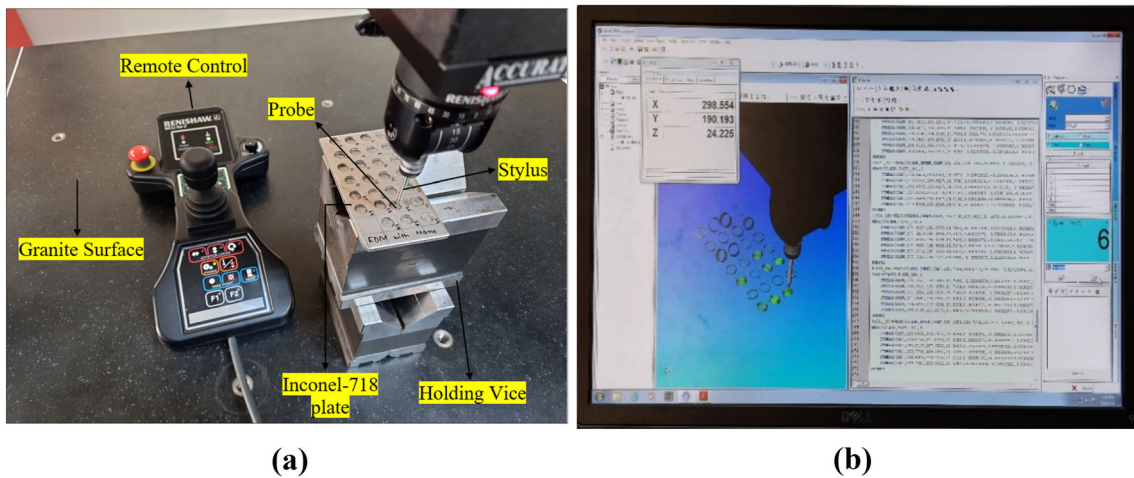


Figure 3. CMM machine measuring form tolerances (a) Probe arrangement for measuring Cylindricity of the hole. (b) ARCOCAD software analysis of Cylindricity.

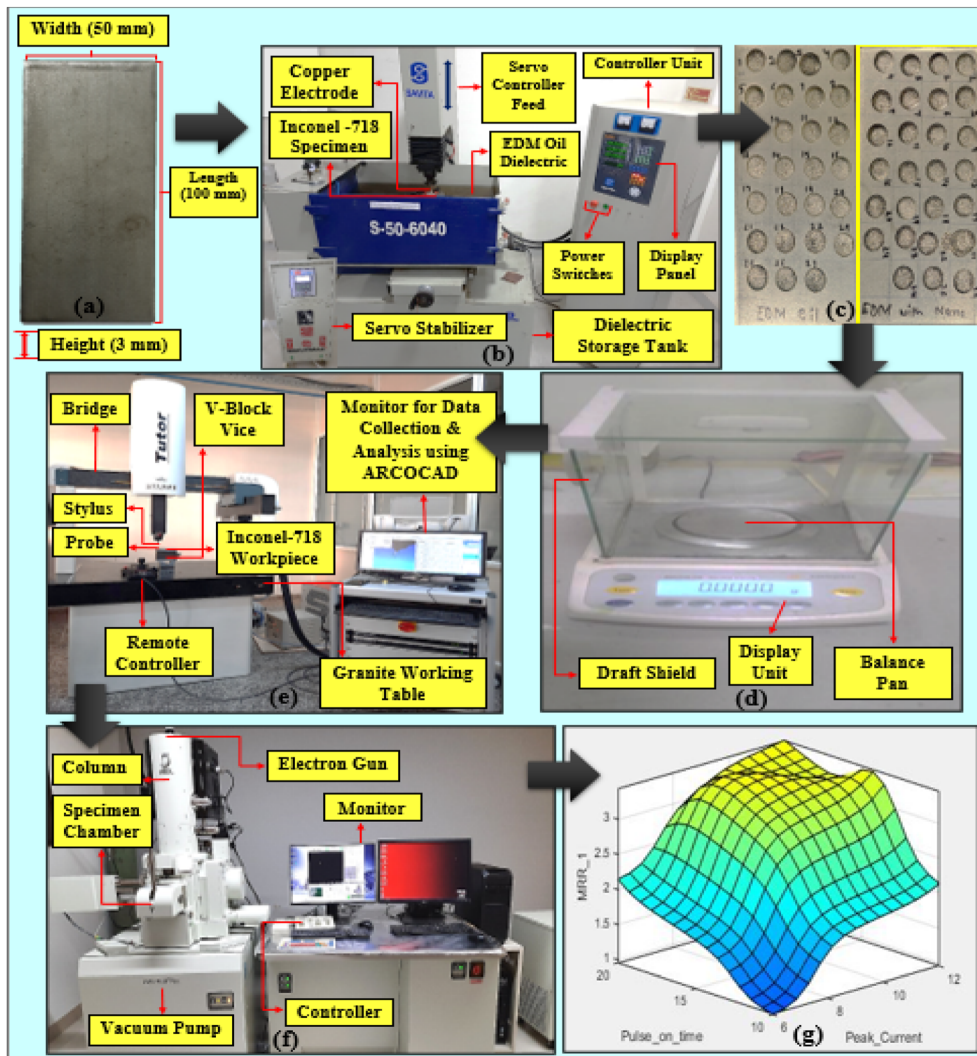


Figure 4. Workflow diagram (a) Specimen (Inconel 718), (b) EDM set up for machining, (c) Holes machined on the workpiece after EDM, (d) Electronic Weighing Balance, (e) CMM set up for measuring form tolerances, (f) FESEM machine to study surface morphology and (g) ANFIS prediction and MOSOA optimization.

Table 4. ANOVA analysis for cylindricity using conventional EDM (CY1).

Source	DF	Seq SS	Adj SS	Adj MS	F-Value	P-Value	Contribution (%)
Pulse on time	2	0.99637	0.99637	0.498183	54.54	0.000	36.52
Pulse off time	2	0.07990	0.07990	0.039948	4.37	0.027	2.93
Peak Current	2	1.46941	1.46941	0.734705	80.44	0.000	53.86
Error	20	0.18268	0.18268	0.009134			6.70
Total	26	2.72835					100.00
		$R^2 = 91.44\%$		$R^2 (adj) = 89.59\%$			

66.12%, respectively. The next significant contribution was for a pulse on time having 36.52% and 23.37% contribution on responses of CY1 and MRR1, respectively. The pulse off time is least significant for both the responses.

The main effect plots for CY1 and MRR1 are shown in figure 5a and b which depict the variation of responses by changing the input variables level. From figure 5a, it has been observed that cylindricity (CL) first decreases with

Table 5. ANOVA analysis for material removal rate using conventional EDM (MRR1).

Source	DF	Seq SS	Adj SS	Adj MS	F-Value	P-Value	Contribution (%)
Pulse on time	2	4.846	4.846	2.42325	43.39	0.000	23.37
Pulse off time	2	1.064	1.064	0.53218	9.53	0.001	5.13
Peak Current	2	13.715	13.715	6.85730	122.79	0.000	66.12
Error	20	1.117	1.117	0.05584			5.38
Total	26	20.742					100.00
		$R^2 = 92.23\%$		R^2 (adj) = 89.21%			

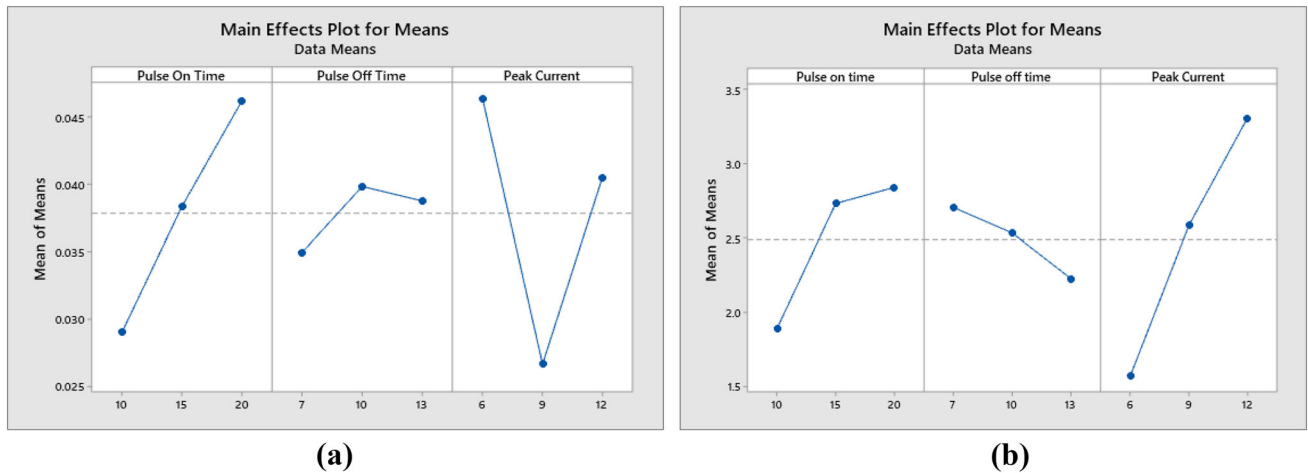


Figure 5. Main effects plot for means using simple EDM (a) CY1, (b) MRR1.

increase in peak current (A) and then augmented with elevation in peak current. In addition, the increase in pulse on time causes enhancement in cylindricity value significantly. The possible reason being higher discharge energy duration with more pulse on time resulting in higher melting and vaporization of material from holes. The minimum cylindricity deviation may be realized at lower level of pulse on time and medium level of peak current. Figure 5b shows the variation of MRR1(mm³/min) with change in input parameters level. Both higher pulse on time and peak current higher values provides augmented MRR value owing to higher discharge energy and better melting and vaporization of material from workpiece. The pulse off

time (μs) increase has negative effect on material removal rate owing to higher time between two sparks, thus resulting in lower discharge energy and hence lower MRR value is realized.

The experimental results for nanographene powder mixed EDM are also reported in table 3, while their corresponding statistical analysis using ANOVA tests were reported for CY2 and MRR 2 in tables 6 and 7, respectively. The higher F and p-value provides the indication of the significance of model and input parameters for responses of CY2 and MRR2 (mm³/min). For 95% significance level, the p-value must be lower than 0.05 to confirm the effectiveness of any input parameters. Table 6 shows

Table 6. ANOVA analysis for cylindricity using nanographene mixed EDM (CY2).

Source	DF	Seq SS	Adj SS	Adj MS	F-Value	P-Value	Contribution (%)
Pulse on time	2	0.013045	0.013045	0.006522	72.52	0.000	58.85
Pulse off time	2	0.000742	0.000742	0.000371	4.12	0.032	3.35
Peak Current	2	0.006579	0.006579	0.003290	36.58	0.000	29.68
Error	20	0.001799	0.001799	0.000090			8.12
Total	26	0.022165					100.00
		$R^2 = 98.92\%$		R^2 (adj) =96.14%			

Table 7. ANOVA for material removal rate using nanographene mixed EDM (MRR2).

Source	DF	Seq SS	Adj SS	Adj MS	F-Value	P-Value	Contribution (%)
Pulse on time	2	5.2873	5.2873	2.64367	34.35	0.000	28.73
Pulse off time	2	0.6476	0.6476	0.32378	4.21	0.030	3.52
Peak Current	2	10.9263	10.9263	5.46314	70.98	0.000	59.38
Error	20	1.5393	1.5393	0.07696			8.37
Total	26	18.4004	5.2873	2.64367	34.35	0.000	100.00
		R ² = 97.84%		R ² (adj) = 94.71%			

that Pulse on time is the most contributing factor with 58.85% for minimizing cylindricity deviation in workpiece holes followed by peak current with 29.68% contribution. Similarly, table 7 shows that peak current dominantly influences the MRR with 59.38% contribution followed by Pulse on time affecting MRR with 28.73%, which is different from the conventional EDM results. In addition, the higher R² value of 98.92% for PMEDM cylindricity result outperformed in comparison to 91.44% for conventional EDM indicates that variability in cylindricity deviation in PMEDM was more efficiently explained by the developed model in comparison to conventional EDM. Furthermore, R² value of 97.84% for PMEDM MRR results is higher than simple EDM R² of 92.23% indicating better fitment of model with experimental data.

The main effect plot shown in figure 5a and b for CY2 and MRR2 shows the variation of responses by changing the input variables level. It can be seen from figure 6a that increase in Pulse on time (μs) have a positive impact on cylindricity deviation. Though the rise in cylindricity deviation is comparatively lower than the value realized from conventional EDM processing. The trend is similar for altering peak current as was with conventional, however the minimum cylindricity deviation is attained by

nanographene mixed EDM. The probable reason being higher thermal conductivity of nanographene particles, thus the capability of faster heat dissipation taking amount of heat away from the sparking zone resulting in the reduction of molten material and solidification shrinkage thus providing exact circular holes with minimum deviation. Figure 6b shows that with an increase in pulse on time and peak current the MRR value increases, however higher peak current provides superior MRR. The main reason is the generation of higher discharge energy at a higher value of pulse on time and peak current owing to more thermal energy which removes the material from the workpiece by melting and vaporizing. The optimal combination of input parameters for minimum cylindricity deviation and maximum MRR are A1B1C2 and A3B1C3 for powder mixed EDM process.

From the reported experimental results in table 3 for both responses a mathematical relationship is established between input process parameters and output machining characteristics. Therefore, the regression models were developed based on multiple regression method, thus formulating quadratic equations for machining responses of CY1, MRR1, CY2 and MRR2 in terms of used input variables. The developed quadratic equations for all the

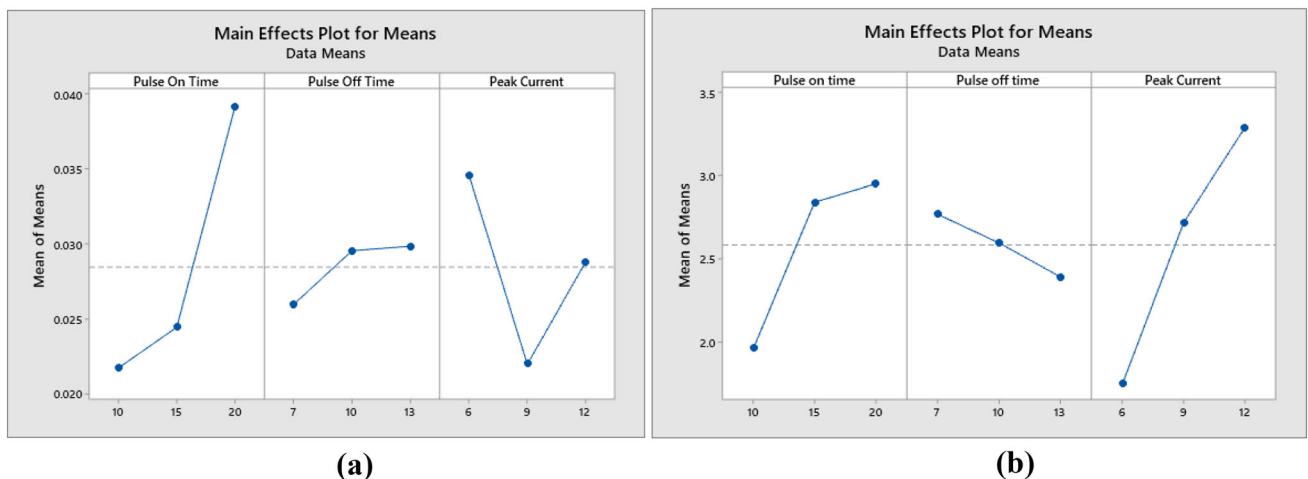


Figure 6. Main effects plot for means using nanographene mixed EDM (a) CY2 and (b) MRR2.

responses under different lubricating environment are shown below:

$$\begin{aligned} \text{MRR1} = & -6.82506 + 0.611000 \text{ Ton} + 0.265679 \text{ Toff} \\ & + 0.902963 \text{ Ip} - 0.001556 \text{ Ton} * \text{ Toff} \\ & - 0.009778 \text{ Ton} * \text{ Ip} - 0.015926 \text{ Toff} \\ & * \text{ Ip} - 0.013756 \text{ Ton}^2 \\ & - 0.008765 \text{ Toff}^2 - 0.017284 \text{ Ip}^2 \end{aligned}$$

$$\begin{aligned} \text{CY1} = & +0.080554 + 0.004464 \text{ Ton} + 0.009843 \text{ Toff} \\ & - 0.032404 \text{ Ip} \\ & - 0.000113 \text{ Ton} * \text{ Toff} - 0.000080 \text{ Ton} * \text{ Ip} \\ & - 0.000094 \text{ Toff} * \text{ Ip} \\ & - 0.000030 \text{ Ton}^2 - 0.000333 \text{ Toff}^2 \\ & + 0.001865 \text{ Ip}^2 \end{aligned}$$

$$\begin{aligned} \text{MRR2} = & -9.03966 + 0.695833 \text{ Ton} + 0.180988 \text{ Toff} \\ & + 0.959537 \text{ Ip} - 0.004611 \text{ Ton} * \text{ Toff} \\ & - 0.009944 \text{ Ton} * \text{ Ip} \\ & - 0.015463 \text{ Toff} * \text{ Ip} - 0.015378 \text{ Ton}^2 \\ & - 0.001790 \text{ Toff}^2 - 0.022160 \text{ Ip}^2 \end{aligned}$$

$$\begin{aligned} \text{CY2} = & +0.123125 - 0.006342 \text{ Ton} + 0.004233 \text{ Toff} \\ & - 0.019906 \text{ Ip} + 0.000061 \text{ Ton} * \text{ Toff} \\ & + 0.000033 \text{ Ton} * \text{ Ip} \\ & - 0.000092 \text{ Toff} * \text{ Ip} + 0.000239 \text{ Ton}^2 \\ & - 0.000183 \text{ Toff}^2 \\ & + 0.001076 \text{ Ip}^2 \end{aligned}$$

4. Modeling of machining characteristics using adaptive neuro-fuzzy inference system (ANFIS) model

After studying and analysing the experimental results, the modelling of response machining characteristics in terms of input process variables was presented using adaptive neuro-fuzzy inference system (ANFIS) model. The ANFIS is a well-recognized logical soft computing technique, integrating the advantages of artificial neural network and fuzzy logic, introduced by Jang in 1993 [45]. The ANFIS intelligence utilizes the learning experience of neural network and knowledge representation in terms of linguistic variables of fuzzy logic. The ANFIS methodology provides solution of complex and non-trivial problems following the Takagi-Sugeno artificial intelligence model. It is a kind of artificial neural network that is useful in performing mapping between the inputs and outputs based on both fuzzy IF-Then rules with appropriate membership functions, characterized by human knowledge, and fixed input-output

data sets for neural network training. Fundamentally, ANFIS consists of five layers or steps which are used to construct the architecture of its inference systems such as fuzzy layer, product layer, normalized layer, defuzzifier layer, and total output layer as represented in figure 7. In this figure, y to z denote input parameters while C_1 to C_n and D_1 to D_n nodes are pointing out the suitable membership functions. The training and testing data determines the performance of neural network and the learning algorithms like (hybrid learning and back propagation) of neural network allots the best suitable values of model parameters. The prime objective of the learning algorithms is to achieve the minimized Root Mean Square Error (RMSE).

The machining experimental results with or without nanographene mixed EDM for both the responses are utilized for training and testing process. In this work, for estimating cylindricity and MRR, the ANFIS model was constructed through MATLAB R20b software considering input as pulse on time (Ton), pulse off time (Toff) and peak current (Ip). In this work, multi-input single output strategy was adopted for prediction of individual machining characteristics, the architecture of ANFIS model based on sugeno fuzzy inference system is shown in figure 8a. The linguistic values of membership functions for individual input parameters are 5 (lowest, low, medium, high, highest) and having 17 rules. Considering this, 17 combinations from the total of 27 combinations were taken as the training data and the remaining 10 combinations were taken as the testing data. The membership functions were utilized for transforming input variables to fuzzy set values. The developed ANFIS model have used Gaussian membership functions for specifying the linguistic inputs. It is to be noted that selection of fuzzy inference system, number of epochs, training and testing data sets were selected based on hit-and-trial technique. The ANFIS training is performed using a hybridization of back propagation algorithm and least square method. The structure of the developed ANFIS model with five layers is shown in figure 8b.

The training and testing plots were generated as shown in figure 9a and b for cylindricity (CY1) data sets considered from individual setting of input parameters without nanographene mixed dielectric. The testing was performed to validate the ANFIS model prediction efficacy in the case of conventional EDM. The sub-clustering FIS system was adopted to get a proper ANFIS model structure. The number of epochs considered were 200 for reducing the error to the minimum, after that value the error shows an increasing trend. During training of data sets, the 17 performance measuring values were used to conduct 100 cycles of learning producing an average training error of 2.1501e-09 for CY1 (without nano graphene EDM), while the testing plots generated with average testing error of 0.0087865. Similarly, figure 9c and d illustrated the MRR1 training and testing plots using conventional EDM. The average training and testing error for MRR1 comes out as 1.6101e-07 and 0.038475, respectively. The training and

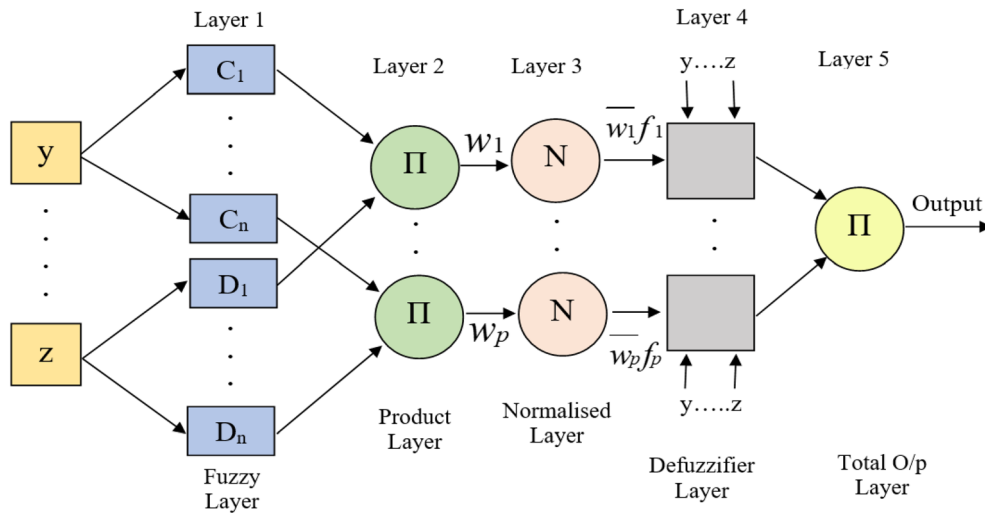
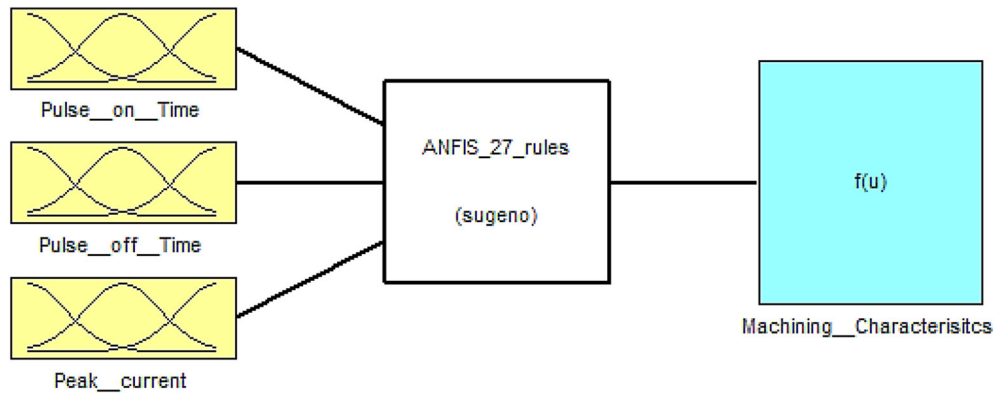
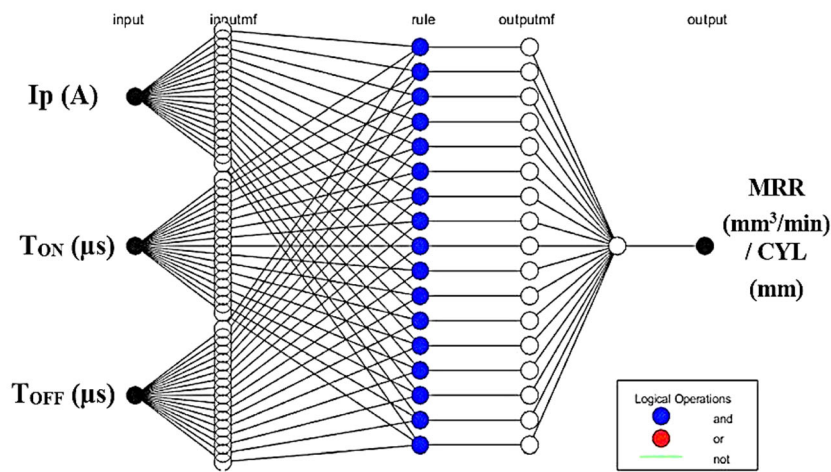


Figure 7. Generalized architecture of Adaptive Network Fuzzy Inference System.



(a)



(b)

Figure 8. The ANFIS (a) model and (b) structure for predicting machining characteristics.

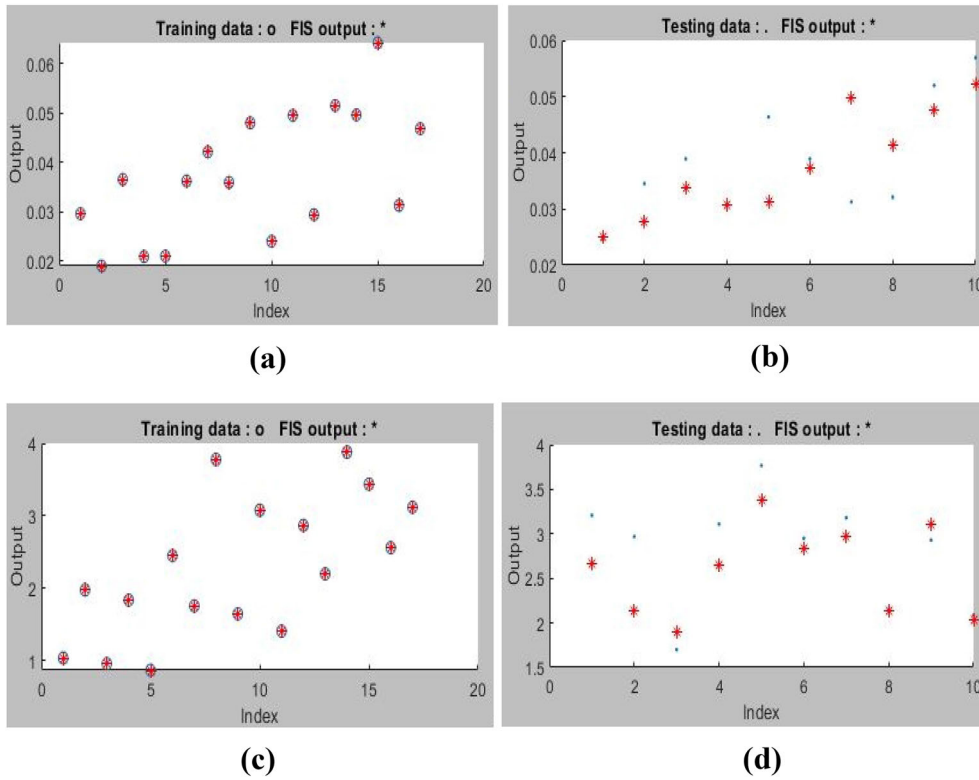


Figure 9. (a) ANFIS model prediction of responses for conventional EDM, (a) cylindricity training, (b) cylindricity testing, (c) MRR1 training and (d) MRR1 testing.

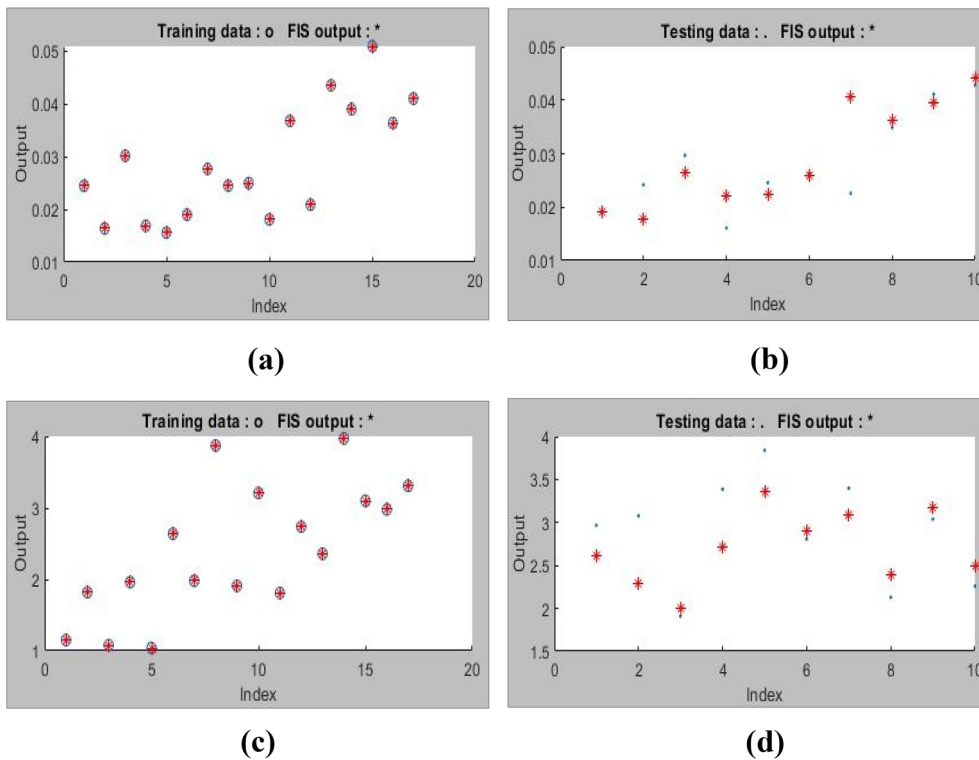


Figure 10. (a) ANFIS model prediction of responses for nano graphene mixed EDM (a) cylindricity training (b) cylindricity testing (c) MRR2 training (d) MRR2 testing.

testing results confirm that the developed ANFIS model are well within the acceptable error range and the results can be used for analyzing the relation between input and output variables in conventional EDM processing of Inconel 718 workpiece.

The results of training and testing the ANFIS model for nanographene mixed dielectric EDM datasets is shown in figure 10a and b depicting training and testing plots generated for cylindricity deviation on different settings of input viz. Peak current (I_p), pulse on time (T_{on}) and pulse off time (T_{off}). The mean training error comes out as $1.2701e-09$ for CY2, while the mean testing error is 0.005462. The training error for cylindricity deviation in case of nanographene mixed EDM is comparatively lower than the training error for without graphene EDM cylindricity, thus showing better results prediction and experimental results also. Figure 10c and d show the training and testing plots generated for MRR2 during nano graphene mixed dielectric machining. The mean training error for material removal rate (MRR2) data comes out as $1.1633e-07$ and mean testing error is 0.41122. Therefore, it is evident that the ANFIS prediction for both the responses is better and more precise in case of

nanographene mixed EDM as compared for conventional EDM prediction.

Figure 11a, b, c, and d show the ANFIS prediction results in comparison to experimental results and regression analysis for corresponding data of response variables viz. CY1 and MRR1 during conventional EDM without nano graphene dielectric processing. From figures 11a and c, it can be inferred that the ANFIS prediction results are in close proximity with the experimental results. Furthermore, for checking the adequacy of the developed model and efficacy of input variables, the diagnostic tests were performed shown in figures 11b and d in terms of normal distribution plots. The distribution level of the measured and predicted data mapped graphically. The normal plots for MRR1 and CY1 for conventional EDM shows that the residual data fall in a straight line validating that errors are normally distributed. It can be illustrated that the cylindricity deviation and material removal rate for conventional EDM has a good correlation with experimentation having correlation coefficient (R^2) value of 0.9177 and 0.9365, respectively.

Figure 12a, b, c, and d depict the ANFIS prediction results in comparison to experimental results and regression analysis for corresponding data of response variables viz.

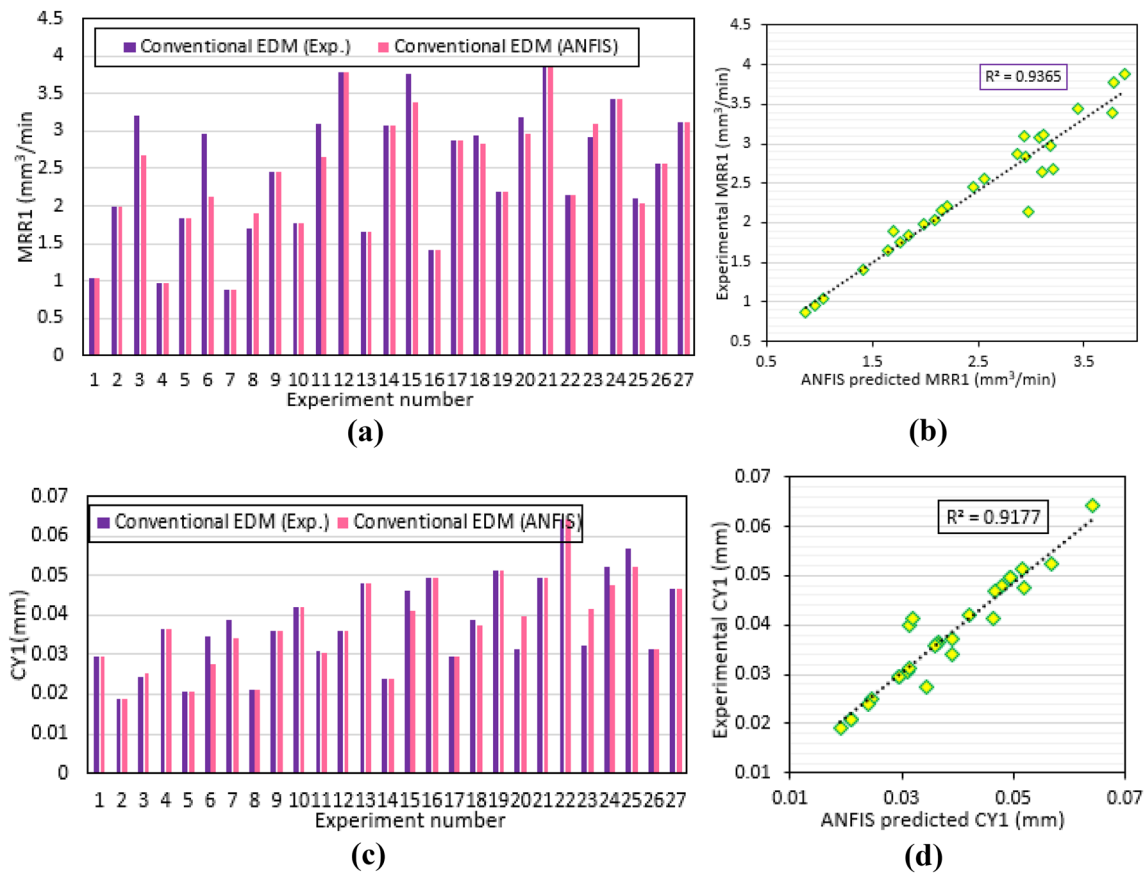


Figure 11. Conventional EDM plot for (a) Comparative results of MRR1, (b) ANFIS model vs experimental results for MRR1, (c) Comparative results of CY1 and (d) ANFIS model vs experimental results for CY1.

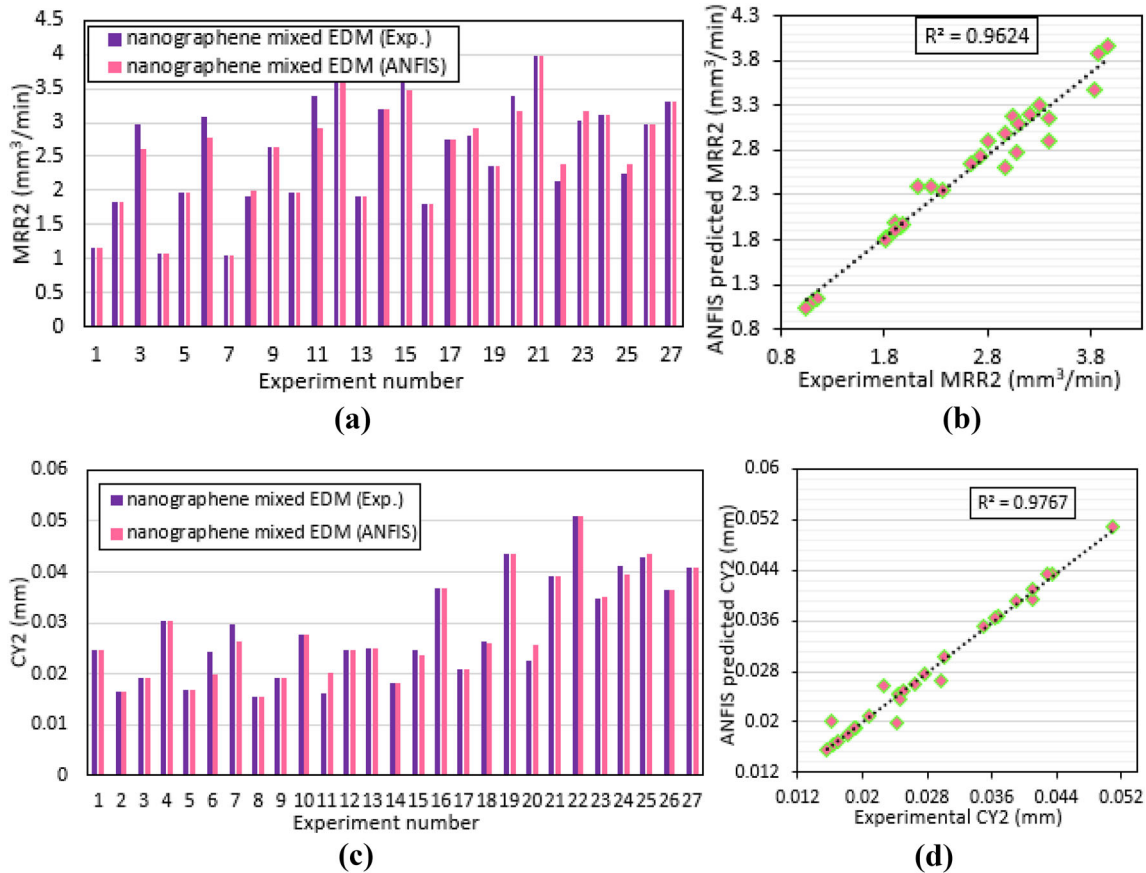


Figure 12. Nanographene mixed EDM plot for (a) Comparative results of MRR2, (b) ANFIS model vs experimental results for MRR2, (c) Comparative results of CY2 and (d) ANFIS model vs experimental results for CY2.

CY2 and MRR2 during nanographene mixed dielectric EDM processing. From figures 12a and c, it can be implied that the ANFIS prediction results are in close proximity with the experimental results. Furthermore, the diagnostic tests were performed as shown in figures 12b and d for investigating the adequacy of developed ANFIS model along with effectiveness of input variables. The distribution level of the measured and predicted data were mapped graphically along the straight line, which confirms that all data are precisely distributed and have a closer relation among them. It was also found that the cylindricity deviation and material removal rate for nanographene mixed EDM has superior correlation with experimentation results in comparison to conventional EDM results having correlation coefficient (R^2) value of 0.9624 and 0.9767, respectively. Thus, the results of ANFIS models show that nanographene mixed EDM responses have outperformed results of conventional EDM and having a strong correlation with experimental results. Therefore, further surface interaction plots of cylindricity deviation and material removal rate responses are shown only using nanographene mixed EDM processing in figures 13 and 14.

Figure 13a, b, and c show the effect of input parameters interactions on cylindricity deviation under nanographene

mixed EDM of Inconel 718 workpiece. Figure 13a reveals that minimum cylindricity deviation is attained for lower pulse on time value combining with medium to higher peak current. While cylindricity deviation is maximum for higher pulse on time and minimum peak current. The lower value of pulse on time controls the sparking in cross-section of electrode as well as its lateral surface, thus minimizing cylindricity deviation in holes. However, at higher value of pulse on time, there is significant amount of spark takes place developing large amount of energy across the lateral surface of electrode thus showing higher values of cylindricity deviation. Figure 13b reveals that lower cylindricity deviation is attained for lower pulse on time combining all values of pulse off time. This trend displays the insignificance of pulse off time as confirmed by ANOVA analysis in prediction of cylindricity. Moreover, figure 13c also shows that the mid to higher value of peak current provide lower deviation of cylindricity in machined holes using nanographene mixed dielectric EDM.

Similarly, the surface plot showing the effect of input parameters interactions on material removal rate under nanographene mixed EDM of Inconel 718 workpiece is illustrated in figures 14a, b, and c. Figure 14a displayed that maximum material removal rate is achieved for higher

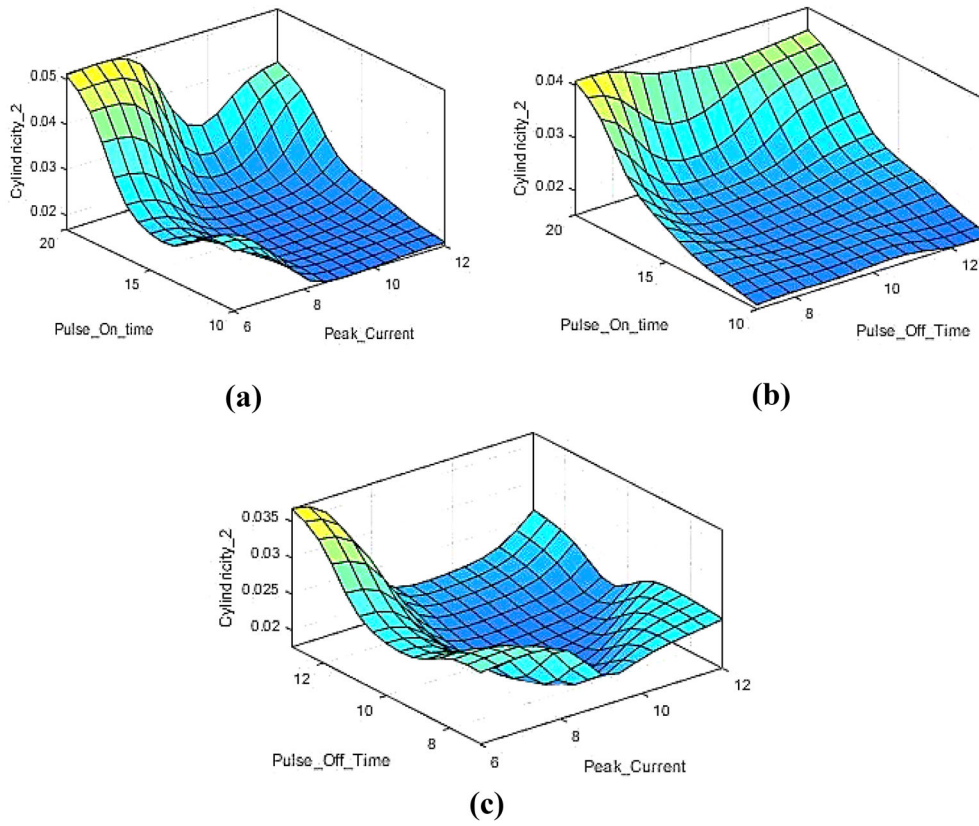


Figure 13. ANFIS three-dimensional plots of Cylindricity for nanographene mixed EDM.

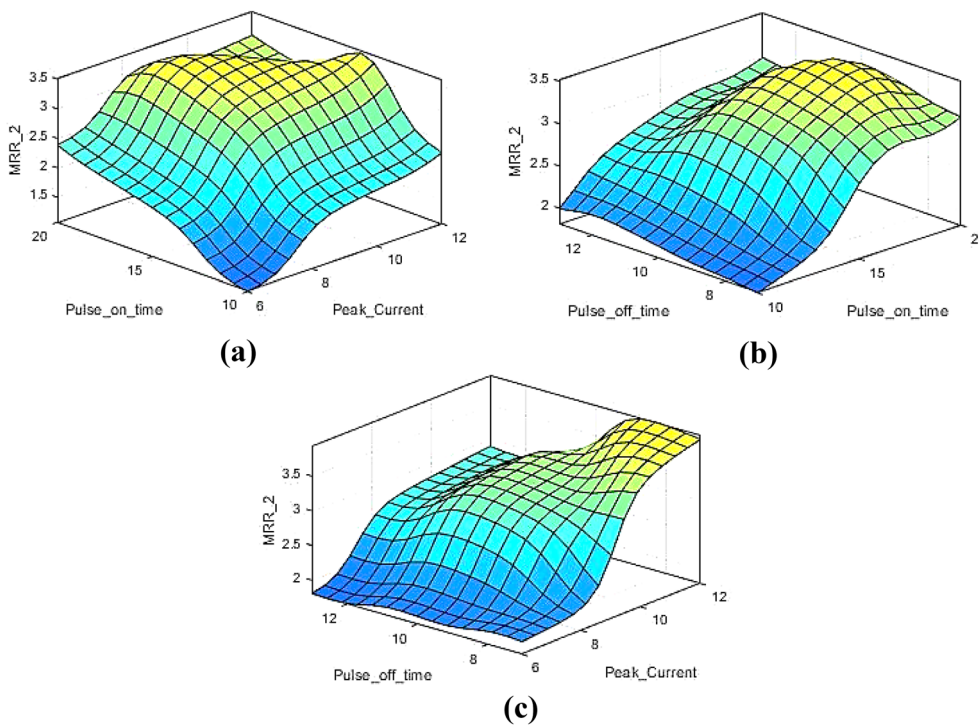


Figure 14. ANFIS three-dimensional plots of MRR for nanographene mixed EDM.

pulse on time value combining with amplifying peak current during nanographene mixed EDM. The primary reason being higher value of both parameters results in more discharging energy and thus supports melting and vaporization of material from the Inconel 718 workpiece. The MRR prediction have least significance of pulse off time as clearly evident from figures 14b and c. From both figures, the pulse off time remains nearly constant with higher values of peak current and pulse on time for realizing higher material removal.

5. Multi-objective optimization of cylindricity and MRR using MOSOA

This section presents application of a newly developed multi-objective Seagull Optimization Algorithm (MOSOA) for minimizing cylindricity deviation and maximizing MRR simultaneously providing best settings of input design variables with or without nanographene mixed EDM processing of Inconel 718 workpiece. The MOSOA was recently developed by Dhiman *et al* [46], which is an advanced version of classical seagull optimization algorithm [47] and aims to find non-dominated pareto optimal solution sets. The classical seagull optimization algorithm mimics the migration and spiral hunting mechanism of seagulls as shown in figure 15. The MOSOA is mainly based on introducing three different concepts in classical seagull optimization algorithm namely dynamic archive for storing the pareto optimal solutions, adaptive grid strategy for excluding the crowded regions in non-dominated solutions and roulette selection mechanism for selecting best solution leader.

For MOSOA, the algorithm begins with initialization of search agents and determining corresponding objective functions. The next step is finding non-dominated solutions and storing them in archive by updating the old solutions. If the archive is full, then remove the most crowded regions using adaptive grid approach and adjust the new solutions

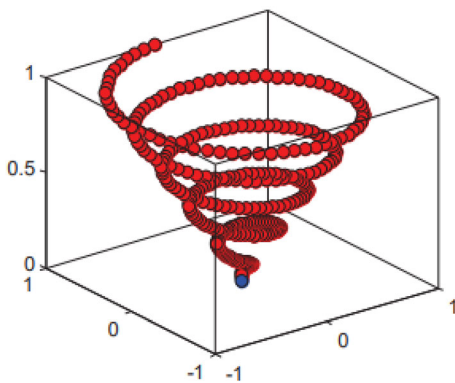
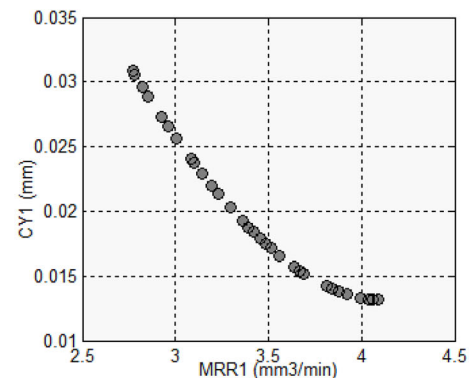


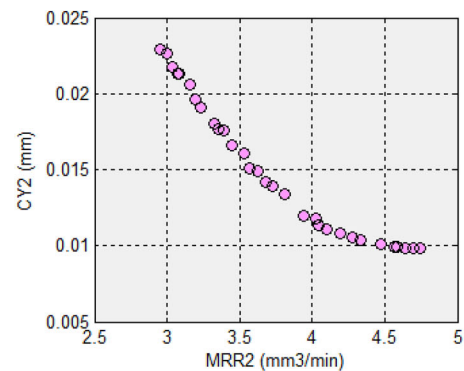
Figure 15. The spiral attacking behaviour of seagulls [46].

to archive. The next step is updating the seagulls from archive based on the updated search agents fitness value. Finally, the stopping criteria is checked, and algorithm stops accordingly by finding the optimal set of solutions. The regression models developed from Equations (1) to (4) are utilized as the objective functions for the MOSOA. The primary objective of the current investigation is to maximize MRR and minimize cylindricity deviation. These objectives are of conflicting nature and functions of peak current, pulse on time and pulse off time as shown in equations (1) to (4) under conventional EDM (MRR1 and CY1) and nanographene mixed EDM (MRR2 and CY2) processing. The search agents or number of seagulls selected were 150 and the stopping criterion is considered as a function tolerance value of 10E-04.

Simultaneous optimization is performed using MOSOA and non-dominated pareto optimal solutions plots with 32 points were generated. The pareto plots having CY vs MRR points with or without nanographene mixed EDM is shown in figure 16a and b. The X and Y axis are displayed as MRR and CY for respective lubricating conditions. The generated 32 feasible points were reported with different setting of input process variables in tables 8 and 9 for conventional and nanographene mixed EDM, respectively. The pareto plots also depict the conflicting nature of two objectives



(a)



(b)

Figure 16. Pareto chart for (a) conventional EDM, CY1 vs MRR1. (b) Nanographene mixed EDM CY2 vs MRR2.

Table 8. Predicted results of MOSOA for conventional EDM.

E. no.	Pulse on time (μs)	Pulse off time (μs)	Peak current (A)	MRR1 (mm^3/min)	CY1 (mm)
1	10.0000	7.0000	6.0000	2.7707	0.0308
2	10.0009	7.0003	7.4057	3.4203	0.0184
3	10.0001	7.0001	9.0319	4.0362	0.0132
4	10.0000	7.0001	6.6630	3.0855	0.0240
5	10.0000	7.0000	6.0000	2.7707	0.0308
6	10.0006	7.0005	7.4802	3.4528	0.0179
7	10.0001	7.0000	8.4172	3.8452	0.0140
8	10.0001	7.0003	6.3985	2.9617	0.0266
9	10.0003	7.0001	6.9031	3.1958	0.0220
10	10.0002	7.0001	8.0326	3.6877	0.0152
11	10.0003	7.0006	6.7968	3.1473	0.0229
12	10.0000	7.0000	6.4952	3.0073	0.0256
13	10.0000	7.0004	6.1762	2.8559	0.0289
14	10.0004	7.0000	7.3425	3.3925	0.0188
15	10.0009	7.0009	7.9760	3.6643	0.0154
16	10.0001	7.0001	8.9666	4.0812	0.0132
17	10.0003	7.0003	8.8000	3.9969	0.0133
18	10.0004	7.0002	6.9802	3.2308	0.0214
19	10.0004	7.0002	7.9169	3.6394	0.0157
20	10.0000	7.0000	7.7262	3.5586	0.0166
21	10.0001	7.0004	6.3193	2.9242	0.0274
22	10.0003	7.0003	8.9111	4.0399	0.0132
23	10.0006	7.0003	8.6022	3.9192	0.0136
24	10.0002	7.0001	6.0218	2.7813	0.0306
25	10.0003	7.0001	8.5084	3.8818	0.0138
26	10.0001	7.0002	7.5626	3.4884	0.0174
27	10.0004	7.0001	7.1235	3.2953	0.0203
28	10.0003	7.0003	6.6983	3.1019	0.0237
29	10.0010	7.0006	8.3329	3.8113	0.0142
30	10.0003	7.0001	7.6223	3.5142	0.0171
31	10.0004	7.0001	7.2784	3.3642	0.0192
32	10.0001	7.0005	6.1099	2.8240	0.0296

and have complementary relationship as one response in inversely proportional to other. Each feasible point of pareto front produced a new set of solution. Based on such variability, one can select the adequate pareto point based on their requirement and conditions. From the pareto graphs, it is evident that cylindricity deviation is found minimum in nanographene mixed EDM in comparison to conventional EDM. Similarly, the MRR is maximized for nanographene mixed EDM and also outperformed conventional EDM values.

Tables 8 and 9 show the results for response variables predicted by MOSOA for conventional and nanographene mixed EDM, respectively. It was observed from table 8 that best values of MRR1 and CY1 were obtained as 4.0812 mm^3/min and 0.0132 mm, respectively, on the corresponding input parameter settings of pulse on time as 10.0001 μs , pulse off time as 7.0001 μs and peak current as 9.0319 A. It was shown in table 9 that the best values predicted by MOSOA for response variables i.e., MRR2 and CY2, are 4.7446 mm^3/min and 0.0098 mm,

respectively, for input parameters setting as: pulse on time of 11.7274 μs , pulse off time of 7.0000 μs and peak current of 9.3696 A. Thus, the results of MOSOA after performing multi-objective optimization of response variables simultaneously show that the nanographene mixed EDM can realize superior results based on better regression modeling and appropriate selection of input parameters. It can also be concluded that the nanographene mixed EDM provide improved MRR and minimum cylindricity deviation by 13.88% and 25.76% respectively in comparison to conventional EDM without nanographene mixed dielectric.

Furthermore, the validation of MOSOA technique results with experimental data have been performed by selecting randomly 7 pareto points from reported 32 feasible non-dominated solution sets. The experimental numbers considered for the validation purpose are 3, 9, 15, 19, 22, 27 and 32 for nanographene mixed EDM processing as it is evident that these results have outperformed conventional EDM results. The experimental and MOSOA predicted values of cylindricity and MRR in the case of nanographene

Table 9. Predicted results of MOSOA for nanographene mixed EDM.

E. no.	Pulse on time (μs)	Pulse off time (μs)	Peak current (A)	MRR2 (mm^3/min)	CY2 (mm)
1	10.0000	7.0000	6.0000	2.9507	0.0230
2	10.0000	7.0000	6.0000	2.9507	0.0230
3	11.7274	7.0000	9.3696	4.7446	0.0098
4	10.3714	7.0015	7.6959	3.8127	0.0134
5	10.1002	7.0044	8.6194	4.0983	0.0111
6	11.6009	7.0002	9.3014	4.6959	0.0098
7	10.1164	7.0002	8.1902	3.9404	0.0120
8	10.7337	7.0026	8.8294	4.3366	0.0104
9	10.4571	7.0003	8.6230	4.1931	0.0119
10	10.2480	7.0011	7.5746	3.7296	0.0139
11	10.0021	7.0013	6.1699	3.0332	0.0217
12	10.0419	7.0006	6.2265	3.0719	0.0213
13	10.0936	7.0035	8.4849	4.0466	0.0114
14	10.2092	7.0005	7.3436	3.6221	0.0149
15	10.2060	7.0000	6.3076	3.1578	0.0206
16	10.1108	7.0001	6.0280	2.9969	0.0227
17	10.0763	7.0004	7.0184	3.4443	0.0166
18	10.0346	7.0014	6.5803	3.2353	0.0190
19	10.1024	7.0013	6.8063	3.3574	0.0177
20	10.1538	7.0014	7.5264	3.6836	0.0142
21	10.0529	7.0018	6.7581	3.3216	0.0180
22	11.1525	7.0002	9.2728	4.5873	0.0099
23	10.2663	7.0007	7.0876	3.5279	0.0161
24	11.2029	7.0009	9.1619	4.5620	0.0100
25	10.6651	7.0018	8.7154	4.2791	0.0106
26	10.6760	7.0010	9.2650	4.4723	0.0101
27	10.1920	7.0014	6.8159	3.3872	0.0175
28	10.0542	7.0008	6.4786	3.1939	0.0197
29	10.1046	7.0000	6.2197	3.0870	0.0213
30	10.0141	7.0022	7.3388	3.5655	0.0151
31	10.4879	7.0021	8.1626	4.0283	0.0118
32	11.4589	7.0020	9.2410	4.6453	0.0099

Table 10. Validation of MOSOA predicted results.

Sl. no.	Pulse on time (μs)	Pulse off time (μs)	Peak current (A)	Optimal		Experimental		Error %	
				MRR2 (mm^3/min)	CY2 (mm)	MRR2 (mm^3/min)	CY2 (mm)	MRR2	CY2
1	12	7	9	4.7446	0.0098	4.3760	0.0108	7.77	8.33
2	10	7	8	4.1931	0.0119	3.9631	0.0131	5.49	9.16
3	10	7	6	3.1578	0.0206	2.8066	0.0226	11.12	8.85
4	10	7	7	3.3574	0.0177	3.1720	0.0194	5.52	8.76
5	11	7	9	4.5873	0.0099	4.1914	0.0110	8.63	10.00
6	10	7	7	3.3872	0.0175	2.9902	0.0182	11.72	3.85
7	11	7	9	4.6453	0.0099	4.3503	0.0107	6.35	7.47

mixed EDM processing are shown in table 10 with the absolute % error. The lower value of error percentages shows that the optimal prediction using MOSOA for material removal rate and cylindricity deviation are in close agreement with the experimental results. The highest error

% for material removal rate is 11.72% while the highest error % for cylindricity deviation is 10%.

The JEOL make Field Emission Scanning Electron Microscope Model (JSM-7610FPlus) has been utilized to investigate the surface quality of holes machined on

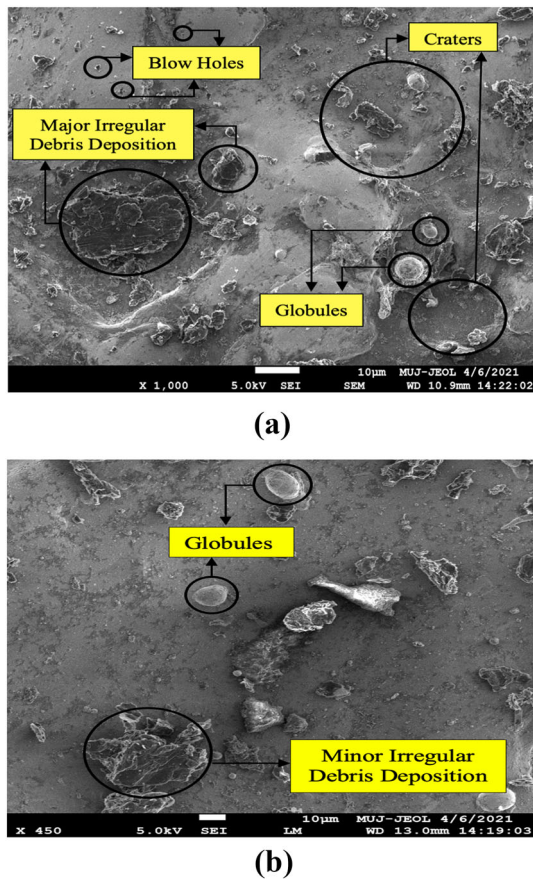


Figure 17. SEM analysis of surface morphology of Inconel 718 specimen. (a) Conventional EDM Oil. (b) Nano graphene mixed EDM.

Inconel-718 specimen through the conventional and nano-graphene mixed EDM. The scanning electron microscopy images are helpful in examining the surface morphology of the machined surface effectively. Figure 17a and b depict the SEM image of machined workpiece surface with or without nanographene mixed EDM for optimum level of input parameters (pulse on time at 12 μ s, Pulse off time at 7 μ s, Peak current at 9 A) from table 10. From figure 17a, it is observed that higher number of craters, micro holes, higher formation of globules, more irregular debris deposition are present on machined surface processing through conventional EDM. In contrast, figure 17b shows significant lower number of pores, globules, cracks, and debris deposition for nanographene mixed EDM processing. The presence of graphene nanoparticles widens the electrode gap due to which the deposition of irregular debris particles was minimal contrary to simple EDM dielectric because of smooth flushing of debris produced results in improved surface finish. The addition of nanoparticles also results in absorption of the heat produced from discharge, reduction in discharge power density, and expulsion forces leading to crater formation that is shallower in nature.

6. Conclusions

The present work investigated the influence adding graphene nanoparticles in EDM dielectric medium on cylindricity deviation and material removal rate, during machining Inconel 718 workpiece. The comparative study of machining quality characteristics were performed with or without nanographene mixed EDM considering three stages as modeling, analysis of results and multi-objective optimization. The following concluding points can be inferred from this work:

1. The results demonstrated that usage of nanographene mixed dielectric improves the EDM machining quality characteristics in terms of cylindricity deviation and material removal rate, in comparison to conventional dielectric EDM, with better smoothing of surface irregularities because of higher gap between electrodes and workpiece, ultimately easing out the process of debris removal.
2. The closer to unity values of correlation coefficient (R^2) revealed that all mathematical regression models for Cylindricity deviation and material removal rate were accurate for conventional and nanographene dispersed EDM. Moreover, the nanographene dispersed dielectric EDM results were more accurate in comparison to conventional EDM results with R^2 of 0.9892 and 0.9742 for CY and MRR, respectively.
3. The regression and ANFIS models were developed for determining the correlation between response variables and studied EDM input parameters. The higher R^2 value (close to unity) confirms that the ANFIS predicted values are in close agreement with experimental results.
4. In addition, the peak current has a maximum contribution of 66.16% and 59.38% in prediction of MRR for conventional and nanographene mixed EDM processing, respectively. In contrast, pulse on time has a maximum contribution of 58.85% for cylindricity deviation prediction in the case of nanographene mixed EDM followed by peak current and pulse off time having the contribution of 29.68% and 3.35%, respectively.
5. A newly developed multi-objective seagull optimization algorithm (MOSOA) provided optimal machining conditions at pulse on time at 12 μ s, Pulse off time at 7 μ s, and Peak current at 9 A. For nanographene mixed EDM, the maximum value of material removal rate achieved was 4.7446 mm^3/min , while the minimum cylindricity deviation as 0.098 mm. Thus, nanographene mixed dielectric provided faster MRR rates and relatively smaller cylindricity deviation in comparison with EDM oil.
6. The realized optimal machining conditions using MOSOA provides wide solutions showing efficacy of soft computing approaches over statistical techniques, therefore provides a sustainable methodology for reducing the environmental hazards and health issues.

For future work, optimization of different performance characteristics like electrode wear rate and form tolerances including perpendicularity, flatness, concentricity, etc. can be performed employing nanographene mixed fluid as a dielectric medium in the EDM process by using the other process parameters. In addition, cylindricity deviation can be optimized by other optimization techniques and experimental work can be carried out by altering the dielectric medium from nanographene mixed fluid to other nanoparticles mixed fluid such as alumina, titanium, silicon nanoparticles, etc.

Abbreviations

EDM	Electrical discharge machining
I_p	Peak current
Ton	Pulse on time
Toff	Pulse off time
MRR	Material removal rate
CL	Cylindricity
FESEM	Field emission scanning electron microscope
CMM	Coordinate measuring machine
ANOVA	Analysis of variance
S/N Ratio	Signal to noise ratio

Acknowledgements

The authors would like to express their sincere gratitude towards the School of Automobile, Mechanical and Mechatronics (SAMM) Engineering, Manipal University Jaipur for extending their support by providing machining and results testing equipment to carry out this research successfully. Furthermore, we would like to acknowledge BSDU Jaipur for providing Coordinate Measuring Machine (CMM) to analyse the form tolerance i.e., Cylindricity.

Declarations

Conflict of interest The authors declare that they have no conflict of interest. All co-authors have seen and agree with the contents of the manuscript and there is no financial interest to report.

References

- [1] Ho K H and Newman S T 2003 State of the art electrical discharge machining (EDM). *Int. J. Mach. Tools Manuf.* 43(13): 1287–1300
- [2] Prakash V, Kumar P, Singh P K, Hussain M, Das A K and Chattopadhyaya S 2019 Micro-electrical discharge machining of difficult-to-machine materials: a review. *Proc. Inst. Mech. Eng. Part B: J. Eng. Manuf.* 233(2): 339–370
- [3] Chakraborty S, Bhattacharyya B and Diyaley S 2019 Applications of optimization techniques for parametric analysis of non-traditional machining processes: a review. *Manag. Sci. Lett.* 9(3): 467–494
- [4] Marashi H, Jafarlou D M, Sarhan A A and Hamdi M 2016 State of the art in powder mixed dielectric for EDM applications. *Precis. Eng.* 46: 11–33
- [5] Katz Z and Tibbles C J 2005 Analysis of micro-scale EDM process. *Int. J. Adv. Manuf. Technol.* 25(9–10): 923–928
- [6] Mandal A and Dixit A R 2014 State of art in wire electrical discharge machining process and performance. *Int. J. Mach. Mach. Mater.* 16(1): 1–21
- [7] Wang Z Y, Rajurkar K P, Fan J, Lei S, Shin Y C and Petrescu G 2003 Hybrid machining of Inconel 718. *Int. J. Mach. Tools Manuf.* 43(13): 1391–1396
- [8] Jahan M P, San Wong Y and Rahman M 2010 A comparative experimental investigation of deep-hole micro-EDM drilling capability for cemented carbide (WC-Co) against austenitic stainless steel (SUS 304). *Int. J. Adv. Manuf. Technol.* 46(9–12): 1145–1160
- [9] D'Urso G and Merla C 2014 Workpiece and electrode influence on micro-EDM drilling performance. *Precis. Eng.* 38(4): 903–914
- [10] Teimouri R and Baseri H 2014 Optimization of magnetic field assisted EDM using the continuous ACO algorithm. *Appl. Soft Comput.* 14: 381–389
- [11] Kibria G, Sarkar B R, Pradhan B B and Bhattacharyya B 2010 Comparative study of different dielectrics for micro-EDM performance during microhole machining of Ti-6Al-4V alloy. *Int. J. Adv. Manuf. Technol.* 48(5–8): 557–570
- [12] Dwivedi A P and Choudhury S K 2016 Effect of tool rotation on MRR, TWR, and surface integrity of AISI-D3 steel using the rotary EDM process. *Mater. Manuf. Process.* 31(14): 1844–1852
- [13] Khatri B C, Rathod P and Valaki J B 2016 Ultrasonic vibration-assisted electric discharge machining: A research review. *Proc. Inst. Mech. Eng. Part B: J. Eng. Manuf.* 230(2): 319–330
- [14] Sabyrov N, Jahan M P, Bilal A and Perveen A 2019 Ultrasonic vibration assisted electro-discharge machining (edm)—An overview. *Materials* 12(3): 522
- [15] Singh J and Sharma R K 2016 Assessing the effects of different dielectrics on environmentally conscious powder-mixed EDM of difficult-to-machine material (WC-Co). *Front. Mech. Eng.* 11(4): 374–387
- [16] Teimouri R and Baseri H 2012 Effects of magnetic field and rotary tool on EDM performance. *J. Manuf. Process.* 14(3): 316–322
- [17] Singh Bains P, Sidhu S S and Payal H S 2018 Investigation of magnetic field-assisted EDM of composites. *Mater. Manuf. Process.* 33(6): 670–675
- [18] Tzeng Y F and Lee C Y 2001 Effects of powder characteristics on electrodischarge machining efficiency. *Int. J. Adv. Manuf. Technol.* 17(8): 586–592
- [19] Kozak J, Rozenek M and Dabrowski L 2003 Study of electrical discharge machining using powder-suspended working media. *Proc. Inst. Mech. Eng. Part B: J. Eng. Manuf.* 217(11): 1597–1602
- [20] Yadav L, Lal S, Singh N K, Chouhan D S and Singh Y 2020 Impact of powder additives in liquid and gaseous dielectric fluids on electrical discharge machining through aerospace region applications—A review. *Mater. Today: Proc.* 25: 952–960

- [21] Mohanty S and Routara B C 2016 A review on machining of metal matrix composites using nanoparticle mixed dielectric in electro-discharge machining. *Int. J. Automot. Mech. Eng.* 13(2): 3518–3539
- [22] Surekha B, Sree Lakshmi T, Jena H and Samal P 2019 Response surface modelling and application of fuzzy grey relational analysis to optimise the multi response characteristics of EN-19 machined using powder mixed EDM. *Aust. J. Mech. Eng.* 19(1): 19–29
- [23] Paswan K, Pramanik A and Chattopadhyaya S 2020 Machining performance of Inconel 718 using graphene nanofluid in EDM. *Mater. Manuf. Process.* 35(1): 33–42
- [24] Baseri H and Sadeghian S 2016 Effects of nanopowder TiO₂-mixed dielectric and rotary tool on EDM. *Int. J. Adv. Manuf. Technol.* 83(1–4): 519–528
- [25] Kumar A, Maheshwari S, Sharma C and Beri N 2010 A study of multiobjective parametric optimization of silicon abrasive mixed electrical discharge machining of tool steel. *Mater. Manuf. Process.* 25(10): 1041–1047
- [26] Sivaprakasam P, Hariharan P and Gowri S 2019 Experimental investigations on nano powder mixed Micro-Wire EDM process of inconel-718 alloy. *Measurement* 147: 106844
- [27] Kumar A, Mandal A, Dixit A R and Das A K 2018 Performance evaluation of Al₂O₃ nano powder mixed dielectric for electric discharge machining of Inconel 825. *Mater. Manuf. Process.* 33(9): 986–995
- [28] Sari M M, Noordin M Y and Brusa E 2013 Role of multi-wall carbon nanotubes on the main parameters of the electrical discharge machining (EDM) process. *Int. J. Adv. Manuf. Technol.* 68(5): 1095–1102
- [29] Yeo S H, Tan P C and Kurnia W 2007 Effects of powder additives suspended in dielectric on crater characteristics for micro electrical discharge machining. *J. Micromech. Microeng.* 17(11): N91
- [30] Prihandana G S, Sriani T, Mahardika M, Hamdi M, Miki N, Wong Y S and Mitsui K 2014 Application of powder suspended in dielectric fluid for fine finish micro-EDM of Inconel 718. *Int. J. Adv. Manuf. Technol.* 75(1–4): 599–613
- [31] Tiwary A P, Pradhan B B and Bhattacharyya B 2019 Influence of various metal powder mixed dielectric on micro-EDM characteristics of Ti-6Al-4V. *Mater. Manuf. Process.* 34(10): 1103–1119
- [32] HuuPhan N, Muthuramalingam T, Vu N N and Tuan N Q 2020 Influence of micro size titanium powder-mixed dielectric medium on surface quality measures in EDM process. *Int. J. Adv. Manuf. Technol.* 109(3): 797–807
- [33] Prabhu S, Uma M and Vinayagam B K 2013 Adaptive neuro-fuzzy interference system modelling of carbon nanotube-based electrical discharge machining process. *J. Braz. Soc. Mech. Sci. Eng.* 35(4): 505–516
- [34] Cogun C, Özerkan B and Karacay T 2006 An experimental investigation on the effect of powder mixed dielectric on machining performance in electric discharge machining. *Proc. Inst. Mech. Eng. Part B: J. Eng. Manuf.* 220(7): 1035–1050
- [35] Abhilash P M and Chakradhar D 2020 Prediction and analysis of process failures by ANN classification during wire-EDM of Inconel 718. *Adv. Manuf.* 8(4): 519–536
- [36] Jafarian F 2020 Electro discharge machining of Inconel 718 alloy and process optimization. *Mater. Manuf. Process.* 35(1): 95–103
- [37] Sengottuvel P, Satishkumar S and Dinakaran D 2013 Optimization of multiple characteristics of EDM parameters based on desirability approach and fuzzy modeling. *Procedia Eng.* 64: 1069–1078
- [38] Ashok R, Poovazhagan L, Srinath Ramkumar S and Vignesh Kumar S 2017 Optimization of material removal rate in wire-EDM using fuzzy logic and artificial neural network. *Appl. Mech. Mater.* 867: 73–80
- [39] Dhanabalan S, Sivakumar K and Narayanan C S 2013 Optimization of machining parameters of EDM while machining Inconel 718 for form tolerance and orientation tolerance. *Indian J. Eng. Mater. Sci.* 20(5): 391–397
- [40] Kumar S and Dhanabalan S 2019 Influence on machinability and form tolerance of Inconel 718 in Edm using different diameter multi hole Cu electrodes. *SN Appl. Sci.* 1(5): 396
- [41] Senthilkumar T S and Muralikannan R 2019 Enhancing the geometric tolerance of aluminium hybrid metal matrix composite using EDM process. *J. Braz. Soc. Mech. Sci. Eng.* 41(1): 41
- [42] Bhaumik M and Maity K 2019 Effect of electrode materials on different EDM aspects of titanium alloy. *Silicon* 11(1): 187–196
- [43] Sandhya M, Ramasamy D, Sudhakar K, Kadirgama K, Samyano M, Harun W S W, Nazafi G, Mofijur M and Mazlan M 2021 A systematic review on graphene-based nanofluids application in renewable energy systems: Preparation, characterization, and thermophysical properties. *Sustain. Energy Technol. Assess.* 44: 101058
- [44] Pathak V K and Singh R 2021 A comprehensive review on computational techniques for form error evaluation. *Arch. Comput. Methods Eng.* 29: 1199–1228
- [45] Jang J S 1993 ANFIS: adaptive-network-based fuzzy inference system. *IEEE Trans. Syst. Man Cybern.* 23(3): 665–685
- [46] Dhiman G, Singh K K, Soni M, Nagar A, Dehghani M, Slowik A, Kaur A, Sharma A, Houssein E H and Cengiz K 2021 MOSOA: a new multi-objective seagull optimization algorithm. *Expert Syst. Appl.* 167: 114150
- [47] Dhiman G and Kumar V 2019 Seagull optimization algorithm: Theory and its applications for large-scale industrial engineering problems. *Knowl.-Based Syst.* 165: 169–196